Regular Article

ANALYTICAL AND BIOANALYTICAL CHEMISTRY RESEARCH

Published by the Iranian Chemical Society

Anal. Bioanal. Chem. Res., Vol. 5, No. 2, 373-386, December 2018.

Response Surface Methodology for Optimization of Green Silver Nanoparticles Synthesized *via* Phlomis Cancellata Bunge Extract

Somayeh Heydari[a,*] and Mohadeseh Hosseinpour Zaryabi[b]

[a]*Department of Chemistry, University of Torbat-e jam, Torbat-e jam, Iran*

[b]*Department of Chemistry, University of Birjand, Birjand, Iran*

(Received 17 March 2018, Accepted 26 June 2018)

Green synthesis of metal nanoparticles is an interesting issue of nanoscience due to its simplicity and eco-friendliness. The present study describes a cheaper, non-toxic and simple route for biosynthesis of Silver nanoparticles using Phlomis cancellata Bunge extracts. Since the experimental conditions of this procedure play vital roles in the synthesis rate of the nanoparticles, a response surface methodology using the central composite design was employed for testing the reaction variables. The individual and interactive effects of process variables (temperature, time, concentration of $AgNO_3$ and pH) on the production rate of AgNPs were monitored and the optimal reaction conditions for the maximum production were found at the reaction temperature of 77.62 °C, duration of 24.79 min, pH of 6.84 and concentration of 4.76 mM of $AgNO_3$. AgNPs were characterized by advanced techniques like UV-Vis spectroscopy (UV-Vis), infrared spectroscopy (IR), scanning electron microscope (SEM) and energy dispersive X-ray spectroscopy (EDX). The weight composition of Ag synthesized by *Phlomis cancellata Bunge* leaf extracts is higher than those normally found in other sources highlighting its industrial application. However, the use of *Phlomis cancellata* leaves can add value to a non-usable waste.

Keywords: Response surface methodology, Green synthesis, Silver nanoparticles, Phlomis cancellata Bunge

INTRODUCTION

Silver Nanoparticles (AgNP) are gaining attention because of wide range of applications in various domains, because they exhibit a large surface area to volume ratio and several unique chemical and physical properties [1]. AgNPs have been used extensively as anti-bacterial agents in the health industry, food storage, textile coatings and a number of environmental applications. Furthermore, the electrochemical properties of AgNPs incorporated them in nanoscale sensors as biological tags that can offer faster response times and lower detection limits. AgNPs are used to efficiently harvest light and for enhanced optical spectroscopies including metal-enhanced fluorescence (MEF) and surface-enhanced Raman scattering (SERS).

The properties and function of the AgNPs are size and shape dependent. Consequently, for a better antibacterial and catalytic activity, a specific control over the shape and size of the nanoparticles is prerequisite, which could be achieved by employing different synthesis methods, reducing agents and stabilizers. So far, various physicochemical procedures have been adopted for the synthesis of AgNPs. However, because of the need of environmental friendly AgNPs, green synthesis methods are favoured for the synthesis of these particles [2].

Biosynthesis is an environment-friendly green chemistry based approach that employs unicellular and multicellular biological entities such as plants [3], actinomycetes [4], bacteria [5], fungus [6], yeast [7] and viruses [8]. Recently, various plant extracts have been employed as the source of electrons and stabilizers for green synthesis of nanoparticles [9,10]. Plant extract contains novel primary metabolites such as monosaccharides [11], proteins [12], enzymes [13], and lipids, or secondary metabolites like polyphenolics [14],

*Corresponding author. E-mail: so_heydari_83@yahoo.com

flavonoids [15], alkaloids and terpenes [16] in which these compounds are mainly responsible for the reduction of ionic into bulk metallic nanoparticles formation. Different plants such as huge [17], Lantana camara L. [16], Tabernaemontana divaricate [18] and walnut green husk [19], *etc*. have been used for the synthesis of AgNPs.

The genus *Phlomis* belongs to Labiatae (Lamiaceae) family with 70 annual and perennial species dispersed in the world, mostly in Asia [20]. In spite of high medicinal value and antibactrial virtue [21], the species of *Phlomis* genus has paid less attention of experts. Phlomis cancellata Bunge that has been known as Gushbarre Irani is a perennial and annual species which is used as medicinal herb [22], and has antibacterial property [23]. The phytochemical analysis of the Phlomis cancellata has done by extracting the essence using Hydrodistilation method that four major elements are identified in the herb essence such as Germacrene-D, β-Caryophyllene, Bicyclogermacrene and β-selinene. Hexadecanoic acid and Germacrene-D compounds are recognized as the main elements in the herb essence [23].

To ensure a maximum yield, minimum time, energy and materials consumption in biochemical reactions, the optimization of the variables involved in the process to select the best conditions is needed. Traditionally, optimization is achieved by monitoring the influence of one factor at a time (OFAT), in which other factors are kept constant except the one being optimized and it involves many experiments. This does not allow the estimation of possible interaction between the studied factors [24]. Therefore, the design of experiment (DOE) methods, based on the multivariate static techniques, are appropriate replacements for OFAT methods to optimize the effective factors on procedures. DOE methods are more precise in estimating the effect of each factor, and are also able to estimate the interaction between factors [25]. One of the efficient statistical techniques which is used excessively in optimization procedures is response surface methodology (RSM). RSM is a collection of statistical procedures, including selection of the proper experimental design, prediction and verification of various polynomial models, generation of contour plots and 3D response surfaces, and finally determination of optimum values for the factors employed to maximize the response criteria used [26].

Therefore, the aim of the present study is to optimize a sustainable biosynthesis of silver nanoparticles by Phlomis cancellata Bunge extract in order to perform a green procedure using RSM and employing a central composite experimental design.

EXPERIMENTAL

Materials and Instrumentation

Leaves of Phlomis cancellata Bunge were collected from Bakharz region of Khorasan state of Iran in April, 2017. Silver nitrate ($AgNO_3$) was purchased from Sigma-Aldrich chemicals Germany and used without further purification. Double distilled deionized water was used throughout the course of this investigation. UV-Vis double-beam spectrophotometer (Photonix Ar 2017, UV-Vis Array) with 1 nm resolution and optical length of 1 cm was used for measuring UV-Vis spectra of AgNPs.

Preparation of Plant Aqueous Extract

To remove debris and other contaminated organic contents, leaves of Phlomis cancellata Bunge were washed with deionized water and dried at room temperature. The dried samples were powdered using a sterilized blade and stored for further analysis. 100 ml double deionized water was added to 1 g finely chopped leaves and boiled at 80 °C for 35 min. The extract was cooled and filtered. The extract was stored at 4 °C and used for the synthesis of silver nanoparticles.

Green Synthesis of Silver Nanoparticles

Synthesis of sliver nanoparticles was prepared by adding of 1 ml of the aqueous extract to 4.76 mM sliver nitrate solution (pH = 6.84) allowed to react at 77.62 °C for 24.79 min in the dark to minimize the photo activation of silver nitrate. The colour change of solution from yellow to brown after 3 min of incubation is indicative of the bio-reduction of Ag^+ ions in the solution to Ag°. The formation of Ag-nanoparticles was also monitored using UV-Vis spectroscopy.

Characterization of Synthesized AgNPs

The surface plasmon resonances (SPR) of the synthesized Ag nanoparticles have been studied using UV-Vis double-beam spectrophotometer (Photonix Ar 2017,

Table 1. EDX Characterization Spectrum Obtained for AgNPs

C	285.2	0.1974	22.34	43.41
N	40.7	0.0351	8.97	14.94
O	159.9	0.0468	21.56	31.45
Ag	2737.8	0.7207	47.13	10.20
		1.0000	100.00	100.00

Table 2. The Levels Employed for the Different Factors Employed by Experimental Investigations

Name	labels	Low level	High level
pH	A	5	7
Temperature (°C)	B	60	90
Time (min)	C	15	30
C_{AgNO3} (mM)	D	1.9	5.5

UV-Vis Array) in the range of 300-800 nm. Field emission scanning electron microscope analysis was carried out in instrument TESCAN Mira3 with acceleration voltage 15 kV. SEM reveals information about the sample including external morphology, chemical composition and crystalline structure and orientation of materials making up the sample. SEM provides detailed high resolution images of the sample by rastering a focused electron beam across the surface and detecting secondary or back scattered electron signal. Elements presented with samples identified by EDX characterization. Fourier transformed infrared (FTIR) spectrum of Phlomis cancellata Bunge extract and AgNPs within the range of 400-4000 cm^{-1} was recorded on Brucker alpha 2 FTIR spectrophotometer. FT-IR analysis was performed to determine the functional groups on Phlomis cancellata Bunge leaves extract and predict their role in the synthesis of Ag nanoparticles. The spectrum gives detail about the vibrations and rotations present in the nanocomposite.

Experimental Design

The biological method is the most desirable and quite well established for the synthesis of nanoparticles. The goal of this work was to obtain uniform and well-dispersed silver nanoparticles using statistical experimental design. A design of experiments is a design for devoting experimental measures to treatment levels and the statistical analysis connected with the design. To this end, we have accomplished the experiments based on the statistical design with attention to main factors involved in a general chemical reduction method.

Response surface methodology is a kind of experimental design methods. A collection of mathematical and statistical techniques helpful for the modeling and analysis of problems in which a response of favorite is influenced by several variables and the objective is to

Table 3. Surface Regression Procedure

Run	Block	Factor1 A:pH	Factor 2 B:Temperature	Factor 3 C:Time	Factor 4 D:C_{AgNO3}	Response1 Absorbance
1	Block 1	7	90	15	1.9	0.32
2	Block 1	5	60	15	1.9	0.16
3	Block 1	5	90	30	5.5	1.25
4	Block 1	6	75	22.5	3.7	0.63
5	Block 1	7	60	15	5.5	0.50
6	Block 1	7	60	30	5.5	0.98
7	Block 1	7	90	30	1.9	0.40
8	Block 1	6	75	22.5	3.7	0.61
9	Block 1	6	75	22.5	3.7	0.62
10	Block 1	5	60	30	1.9	0.28
11	Block 1	5	90	15	5.5	0.73
12	Block 1	5	75	22.5	3.7	0.61
13	Block 2	6	75	22.5	5.5	1.29
14	Block 2	6	90	22.5	3.7	0.99
15	Block 2	4	75	22.5	3.7	0.51
16	Block 2	6	75	22.5	1.9	0.10
17	Block 2	6	75	22.5	3.7	0.62
18	Block 2	6	75	22.5	3.7	0.66
19	Block 2	6	75	30	3.7	0.75
20	Block 2	6	60	22.5	3.7	0.43
21	Block 2	8	75	22.5	3.7	0.56
22	Block 2	6	75	22.5	3.7	0.63
23	Block 2	6	75	15	3.7	0.14

optimize this response is defined as response surface methodology (RSM). The main idea of RSM is to use a sequence of designed experiments to obtain an optimal response. If the fitted surface is a sufficient approximation of the true response function, then analysis of the fitted surface will be nearly equivalent to analysis of the real system. RSM was produced using Design- Expert 7.1.5 Trial software.

Table 4. The ANOVA Results of the Quadratic Model

Source	Sum of Squares	Degree of Freedom	Mean Square	F-Value	P-Value	
Block	0.001551	1	0.001551			
Model	2.162743	14	0.154482	926.7244	< 0.0001	Significant
A-pH	0.00125	1	0.00125	7.498661	0.0290	
B-Tem.	0.1568	1	0.1568	940.632	< 0.0001	
C-Time	0.366025	1	0.366025	2195.758	< 0.0001	
D-C_{AgNO3}	0.70805	1	0.70805	4247.542	< 0.0001	
AB	0.0004	1	0.0004	2.399572	0.1653	
AC	0.0008	1	0.0008	4.799143	0.0646	
AD	0.007225	1	0.007225	43.34226	0.0003	
BC	0	1	0	0	1.0000	
BD	0.0064	1	0.0064	38.39314	0.0004	
CD	0.08	1	0.08	479.9143	< 0.0001	
A^2	0.017702	1	0.017702	106.1959	< 0.0001	
B^2	0.00931	1	0.00931	55.85007	0.0001	
C^2	0.063051	1	0.063051	378.2377	< 0.0001	
D^2	0.0059	1	0.0059	35.39566	0.0006	
Residual	0.001167	7	0.000167			
Lack of Fit	2.52E-05	2	1.26E-05	0.055201	0.9469	not significant
Pure Error	0.001142	5	0.000228			
Core Total	2.165461	22				
R-Squared			0.99946076			
Adj R-Squared			0.99838227			
Pred R-Squared			0.99819933			
Adeq Precision			110.506479			
C.V.%			2.15653764			
Std. Dev.			0.0129111			
Mean			0.59869565			
PRESS			0.0038965			

Central Composite Design

Central composite design (CCD) represents a good choice among the standard designs used in RSM, because of its high efficiency with respect to the number of required runs. CCD is to augment a full factorial design by adding so-called star points (set points) and some number of replicate measurements at the center (center points). By spacing all the points at an equal distance from the center, a rotatable design is obtained that gives each point equal leverage in the estimation of the regression coefficients. So, the number of experiments decreases. In this study, the effect of four factors, concentration of $AgNO_3$, pH level, reaction time and temperature, on the biosynthesis of silver nanoparticles was investigated. The investigated factors and their domains are presented in Table 2. The experiments were performed in two blocks of 23 sets of test conditions at five levels with one replicate, and operated in a randomized arrangement to avoid systematic bias. The data analysis is carried out for each response variable described in the following sections as shown in Table 3.

The response surface models were fitted by means of least squares calculation using the following second-order polynomial equation,

$$Y = b_0 + \sum_{i=1}^{n} b_i X_i + \sum_{\substack{i=1 \\ j>i}}^{n-1} \sum_{j=2}^{n} b_{ij} X_i X_j + \sum_{i=1}^{n} b_{ii} X_i^2$$

where Y is the response variable supposed to be modelled, X_i and X_j define the independent variables, b_0 is the constant coefficient, b_i is the coefficient of linear effect, b_{ij} is the coefficient of interaction effect, b_{ii} is the coefficient of quadratic effect, and n is the number of variables.

Figure 6 shows 3D response surfaces and contour plots of the model. The responses were mapped against two experimental factors while the other factors are held constant at its central level. The adequacy of each model was checked using the F-values, lack of fit, and R^2-values, and finally a quadratic model was adopted. The statistical significance of the full quadratic models predicted was considered by the analysis of variance (ANOVA). The ANOVA results of the quadratic model are summarized in Table 4.

RESULTS and DISCUSSION

Biosynthesis of Silver Nanoparticles

Generally, the phytochemicals and phenolics present in the *Phlomis cancellata Bunge* extracts assist the synthesis of the AgNPs. The bio-molecules such as flavonoids, terpenoids, and phenolic compounds present in Phlomis cancellata are responsible for the reduction of silver ions to AgNPs. Hexadecanoic acid, germacrene D, eudesmol, octacosane, (*E*)-caryophyllene, heptacosane, pentacosane, α-copaene and sesquiterpene are major components in *P. cancellata* Bunge extract. The synthesis of AgNPs can be explained in terms of the organic acids and heterocyclic compounds in the plant extract [23]. These play a key role in the synthesis process and can directly reduce Ag ions. In aqueous solution, silver nitrate dissociates into negative nitrate anions and positive Ag^+ cations as given in Fig. 1. The hydrated electrons from aqueous leaf extract of *Phlomis cancellata Bunge* reduce Ag^+ cations into zero valent silver (Ag°) by nucleation process. The higher amounts of biomolecules assist to stabilize the growth of the nanoparticles and hamper particle agglomeration.

Characterization of Silver Nanoparticles

UV-Vis spectrophotometry. It is known that UV-Vis spectroscopy is the most widely used technique for characterizing noble metal nanoparticles exhibiting SPR in the visible range. The SPR property is attributed to the collective oscillation of electrons on the surface of metal nanoparticles excited by external energy source. Thus, the characteristic plasmon peak gives an account of physical nature of the AgNPs. Figure 2 shows the UV-Vis absorption spectra of the synthesized silver nanoparticles in Phlomis cancellata Bunge extract before and after synthesis. Typical exciton absorption at 428 nm was observed at room temperature. A single SPR band is expected to appear in the case of spherical nanoparticles and two or more SPR bands with anisotropic particles [27]. According to Evanoff and Chumanov, 2005, the maximum wavelength and width of the SPR are mainly dependent on the size and shape of the nanoparticles [28]. The broadness of the bandwidth indicates the size of the nanoparticles. Therefore, increased bandwidth in Fig. 2 evidences the

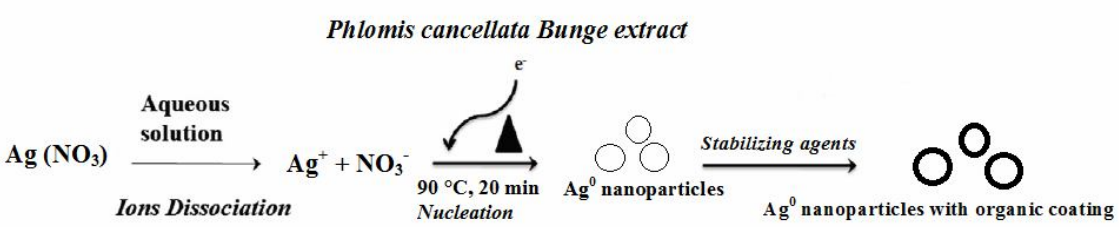

Fig. 1. AgNPs synthesis mechanism using *Phlomis cancellata Bunge* leaves extracts.

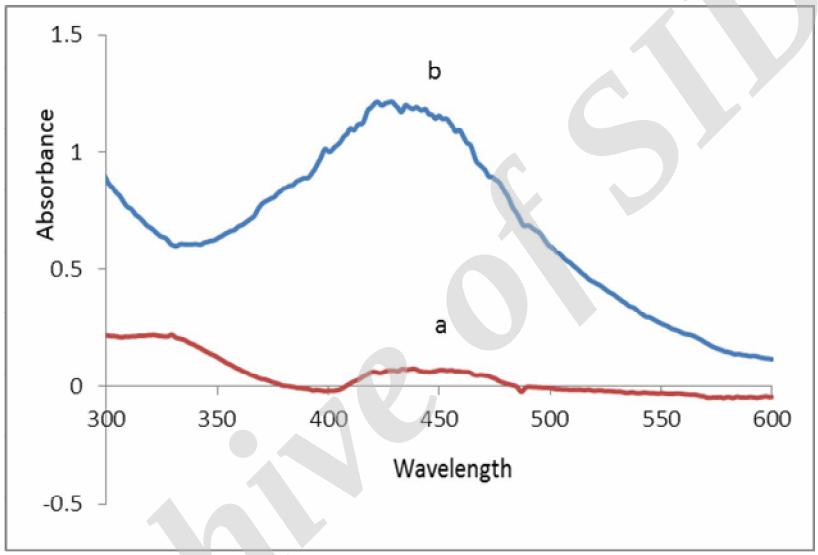

Fig. 2. UV-Vis absorption spectrum of Ag nanoparticles, (a) extract (b) extract with Ag.

presence of smaller particle size of nanoparticles. The size of AgNPs was calculated using the following equation [29],

$$d = \frac{hvf}{\frac{\pi \Delta E1}{2}}$$

where d is the diameter of the particle, h is the Planck's constant, v_f (1.39 × 106 m s^{-1}) is the Fermi velocity of electrons in bulk silver and $\Delta E_{1/2}$ is the full width at half maximum (FWHM) of the absorption band. The sizes of the obtained AgNPs were calculated from the absorption spectra using the equation. The minimum sizes of AgNPs synthesized using *Phlomis cancellata* extract came out to be about 12 nm.

SEM and EDX analyses. SEM micrograph for the biosynthesized AgNPs obtained by mediation of *Phlomis cancellata Bunge* is represented in Fig. 3. It is clearly evident that all these NPs were well separated from each other suggesting that the AgNPs were free from aggregation and spherical. The SEM image of AgNPs shows that the shape of particles is spherical and their size ranges between 10 and 30 nm. To further understand the synthesis of AgNPs, the existence of silver element in the biosynthesized AgNPs was confirmed by EDX as exhibited in Fig. 4, which contains intense peaks of C, O, N and Ag, confirming the presence of Ag. The C, and O signals are attributed mainly to the polyphenol groups and other C, N, O-containing molecules in *Phlomis cancellata Bunge* leaf extracts [23]. Specifically, the C, N, O and Ag loading of AgNPs is 22.34 wt%, 8.97 wt%, 21.56 and 47.13 wt%, respectively (Table 1). The weight composition of Ag

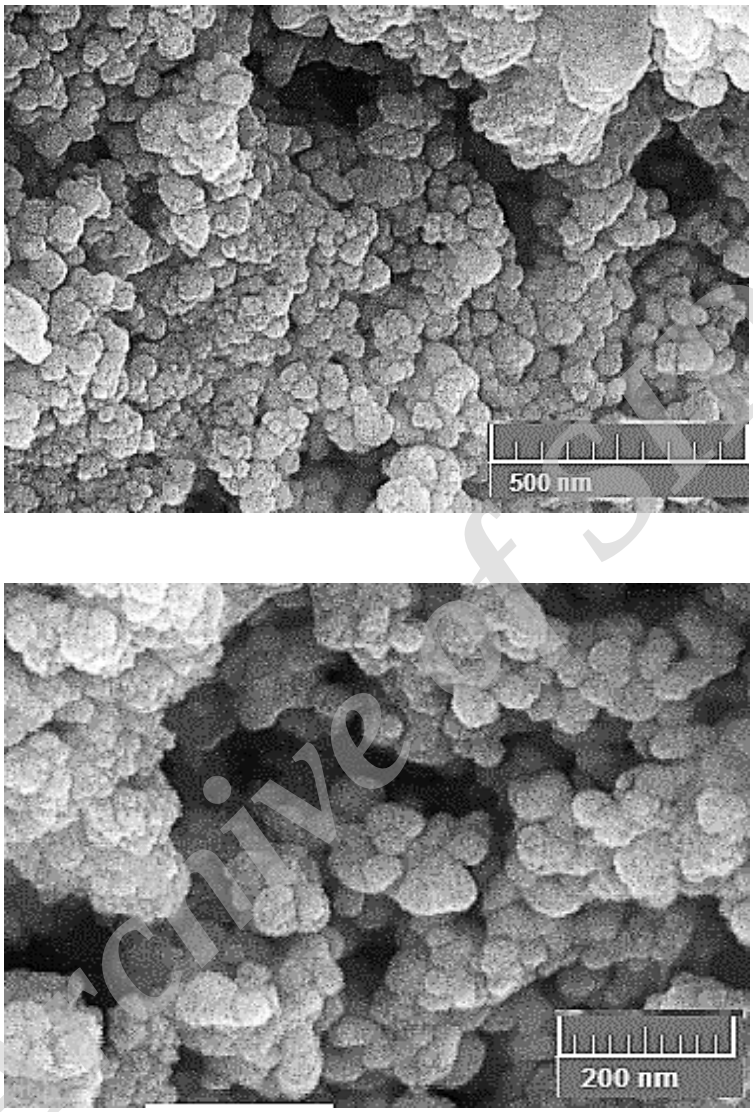

Fig. 3. SEM image of silver nanoparticles on 500 nm and 200 nm scales.

synthesized by *Phlomis cancellata Bunge* leaf extracts is more than that of green Carica papaya leaf extracts whose percentage reported to be 41% [30]. This is because *Phlomis cancellata* has the higher phenolic content than Carica papaya leaves.

FTIR spectroscopy. The binding properties of Ag nanoparticles using Phlomis cancellata Bunge extract were investigated by FTIR spectroscopic analysis. The functional groups may be responsible for AgNPs biosynthesis, stabilization, and capping. The FTIR spectrum of Phlomis cancellata Bunge extract and AgNPs produced by Phlomis cancellata Bunge mediation was represented in Fig. 5. From the spectrum, the peaks observed in the region between 1000 and 1700 cm^{-1} can be assigned to hydroxyl and carbonyl groups and –C-O and -C-O-C stretching modes. On the other hand, methoxy, methylene, and methyl groups stretching vibrations *via* C-H could be detected at 2919, and 2851 cm^{-1}, whereas stretching of O-H in flavonoids, alcohols, and phenols was observed at 3404 cm^{-1}. The peak observed at 533 cm^{-1} is assigned to Ag nanoparticles.

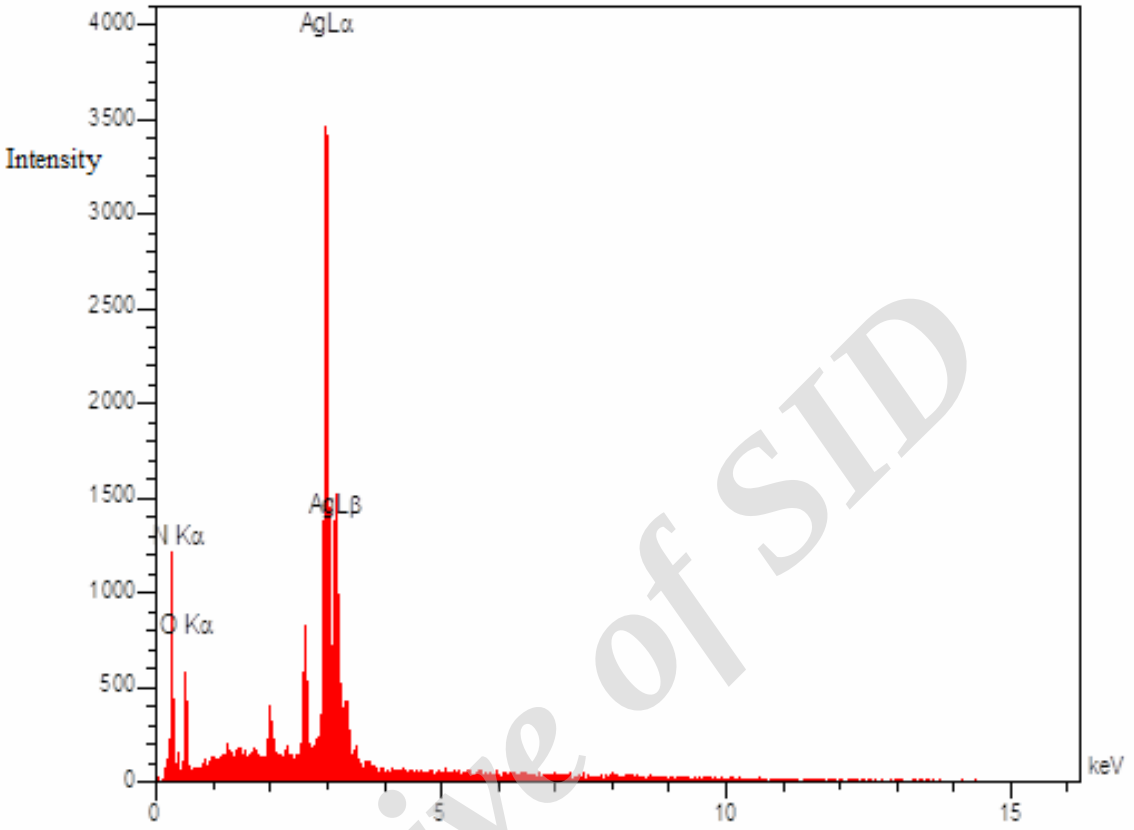

Fig. 4. EDX spectrum obtained for AgNPs.

Response Surface Methodology and Selection of Optimum Conditions

Synthesis of small sized monodispersed nanoparticles is generally dictated by the optimum conditions such as pH, temperature, time of reaction, and concentration of $AgNO_3$. Thus, in order to determine the optimum conditions, the aforementioned parameters were optimized with help of RSM design. The regression model symbolized in the figure of three dimensions surface plots was illustrated to demonstrate the effects of the four studied factors, and collective effects of every independent changeable factor on AgNPs biosynthesis in values of absorbance at 428 nm as indication for AgNPs surface plasmon resonance.

Figures 6a, c and e show that the increase in temperature speeds up the rate of AgNPs biosynthesis reaction. At 77.62 °C, the maximum absorbance was observed, indicating the formation of Ag nanoparticles at high and fast rate leading to formation of smaller size nanoparticles. Earlier reports indicate that at higher temperatures silver ion reduction is favorable and proceeds at higher rate [31]. Figures 6a-c and f explain that by increasing the reaction time, biosynthesis yield increases to extent limit depending on the second tested variable. Optimization revealed 24.79 min as the ideal time, between the minimum of 15 min and maximum of 30 min. Figures 6d-f demonstrate that silver nitrate concentration has a strong significance on AgNPs biosynthesis yield. Since there is a correlation between Ag^+ concentration and the quantity of biomolecules present in reaction medium to get the proper balance for AgNPs biosynthesis, silver nitrate concentration affects silver nanoparticle synthesis significantly. When silver nitrate concentration increased, the AgNPs biosynthesis increased clearly and affected by the interaction of second parameter pH, temperature, and the time of reaction. On increasing the concentration of silver nitrate, a blue shift in the absorption band to the

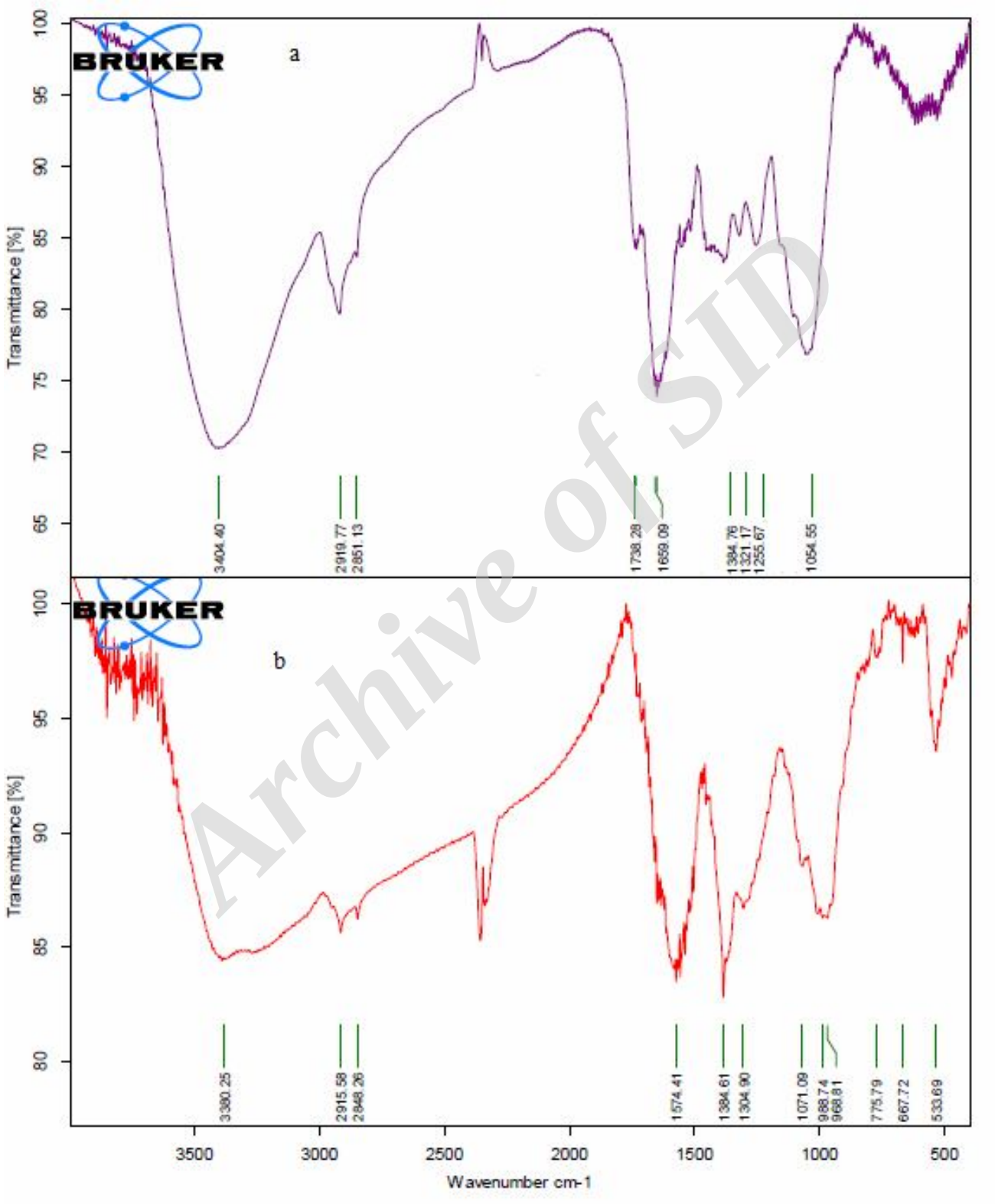

Fig. 5. FTIR spectrum of Ag nanoparticles, (a) extract, (b) extract with Ag.

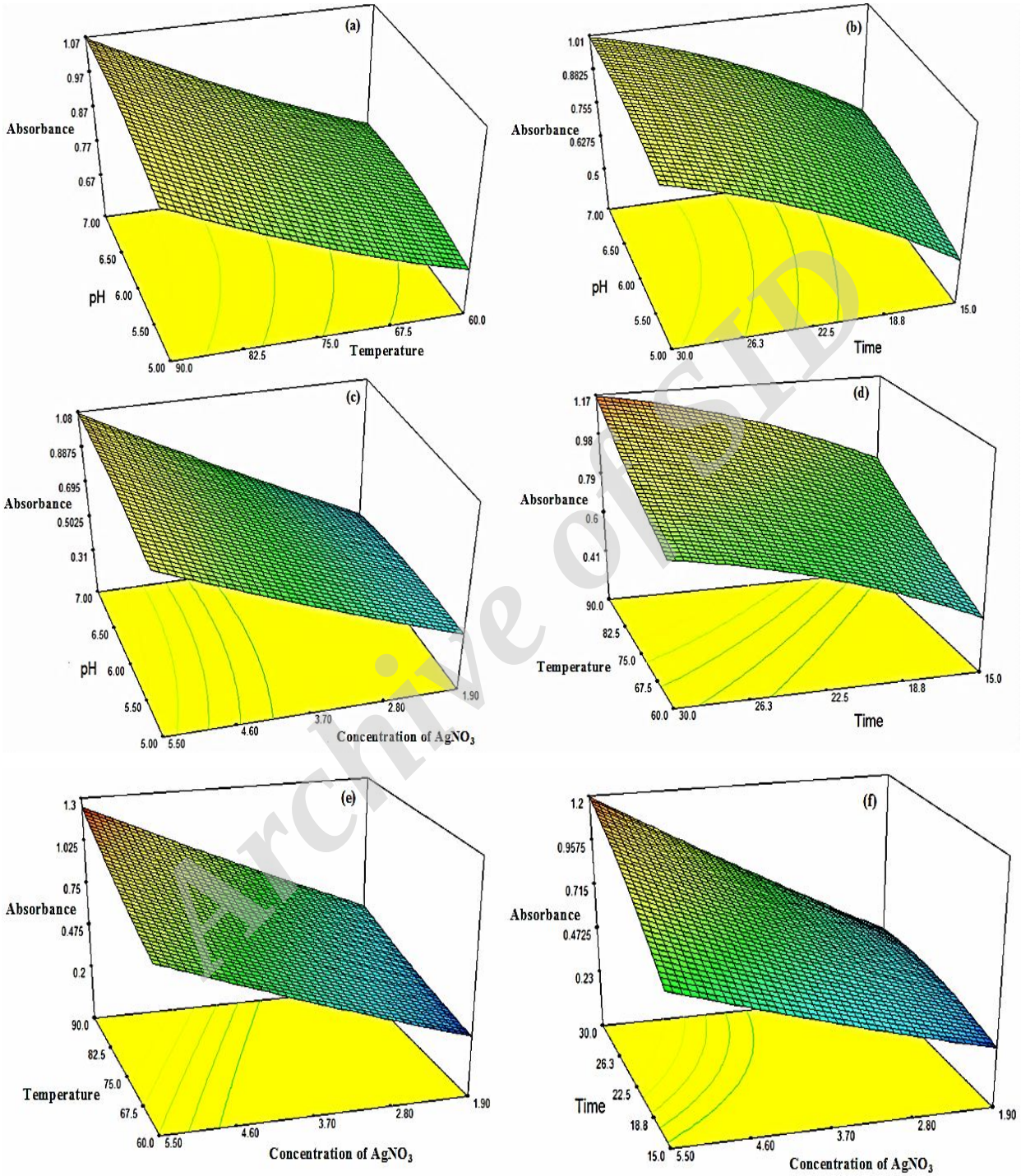

Fig. 6. Estimated response surfaces with related contours by plotting absorbance *versus* (a) pH (A) and Temperature (B); (b) pH (A) and Time of reaction (C); (c) Temperature (B) and Time of reaction (C); (d) pH (A) and $AgNO_3$ concentration (D); (e) Temperature (B) and $AgNO_3$ concentration (D); (f) Time of reaction (C) and $AgNO_3$ concentration (D).

Table 5. Optimization Level of Parameters

pH	Temperature (°C)	Time (min)	C_{AgNO3} (mM)	Response		Error
				Predicted	Experimental	
6.84	77.62	24.79	4.76	0.90842	0.81012	0.015

shorter wavelength (from 440 to 425 nm) was observed, indicating that the particle size is decreasing. In addition to the spectral shift, there was an increase in the absorption intensity with increase in pH. Further, it was observed that higher concentration enhances the rate of reduction as the colour of the solution changed to dark brown more quickly compared to a solution of lower concentration. Hence, $AgNO_3$ at a concentration of 4.76 mM is favorable for the synthesis of AgNPs. Figures 6a, b and d show that the reaction pH has had a lesser momentous outcome on the AgNPs biosynthesis than the effects of other three variables. The results show that with the increase in pH value from 5.0 toward neutral pH values, the AgNPs biosynthesis yield is increased, which is in agreement to previous findings with extracellular fungal [32]. The maximum AgNPs synthesis was achieved at pH 6.84, indicating the potential use of Phlomis cancellata Bunge.

Explanation of Regression Analysis

To find the most suitable fitting of the experimental data, a response surface model was developed using the regression analysis by considering different combinations of the linear, quadratic and interaction terms in polynomial equations which may be expressed as the following equation,

$$R = -0.36332 + 0.20945 \times A - 0.012409 \times B + 0.039047 \times C - 0.28761 \times D + 0.023611 \times A \times D + 1.48148E\text{-}003 \times B \times D + 7.40741E\text{-}003 \times C \times D - 0.025359 \times A^2 + 8.17361E\text{-}005 \times B^2 - 8.50833E\text{-}004 \times C^2 + 4.51871E\text{-}003 \times D^2$$

where R is the obtained absorbance (428 nm) as indication for surface plasmon resonance, A is the reaction pH value, B is the reaction temperature, C is reaction incubation time, and D is the silver nitrate concentration.

The adequacy of the model developed was evaluated based on the correlation coefficient R^2 and standard deviation value. The closer the R^2 value of unity and the smaller the standard deviation implying more accurate response and repeatability that could be predicted by the model [33]. According to Table 4, R^2 and R^2-(adj.) for the model obtained were 0.9995% and 0.9984%, respectively. This confirms that 99.95% of variation can be explained by the fitted model.

Finally, the model was used to predict both the optimum value and optimum region of the factor level, which results in maximum. The model can be considered a practical model for the prediction of the factors used and within the ranges tested. An experimental run was carried out using the optimum combination of parameters and the response was found and listed in Table 5. The results indicate a good agreement between the Predicted and Experimental response which demonstrate the high performance of the model.

The low value of coefficient of variation (2.16) indicates good precision and reliability of the experiments. The adequate precision (110.506) measures the signal to noise ratio and a ratio greater than 4 is generally desirable. Table 4 presented p-value of the variables included in the model. The values of "Prob > F" less than 0.05 indicate the model terms are significant. It can be concluded from Table 4 that three main variables, *i.e.* temperature, time and the concentration of $AgNO_3$, and quadratic terms of them are clearly significant. The interactions between the concentration of $AgNO_3$ with the other three factors (pH, temperature and time) and the interactions between the pH and the time are statistically significant. While the interaction between the temperature with the pH, and the time is statistically insignificant. Also, according to the greater F-value (4247.542), the concentration of $AgNO_3$ is the most important variable of the response. The results

illustrate that the effects of the four studied factors on the AgNPs biosynthesis were dissimilar, and their influence was ordered as D > C > B > A, respectively. As seen, the F-value of lack of fit (LOF) of 0.055201 indicated that the LOFs are not significant relative to the pure errors. The small difference between the yield predicted by the model, and the experimental results, the variance analysis of the model and the insignificant lack of fit, all indicate that the accuracy and fitness of the model was highly satisfactory.

CONCLUSIONS

In this work, using an optimized green synthesis procedure, we successfully obtained a high biosynthesis yield of 47.13% for AgNPs. Through application of response surface methodology using the central composite design, the models were established to identify the effects of pH, temperature, time and concentration of $AgNO_3$, as four effective parameters on the production rate of Ag-nanoparticles using Phlomis cancellata Bunge extract. These ecofriendly, cost effective, stable nanoparticles biosynthesized can be used as an economic and valuable alternative for the large-scale production of Ag nanoparticles.

ACKNOWLEDGEMENTS

The authors acknowledge the financial support of this work by University of Torbat-e jam, Torbat-e jam, Iran.

REFERENCES

[1] T.V. Mathew, S. Kuriakose, Mater. Sci. Eng. C Mater. Biol. Appl. 33 (2013) 4409.
[2] J.A. Dahl, B.L.S. Maddux, J.E. Hutchison, Chem. Rev. 107 (2007) 2228.
[3] P. Rauwel, S. Kuunal, S. Ferdov, E. Rauwel, Adv. Mater. Sci. Eng. 2015 (2015) 1.
[4] S. Abdeen, S. Geo, S. Sukanya, P.K. Praseetha, R.P Dhanya, Int. J. Nano Dimens. 5 (2014) 155.
[5] S. Iravani, Int. Sch. Res. Notices 2014 (2014) 1.
[6] K. Salahuddin Siddiqi, A. Husen, Nanoscale Res. Lett. 11 (2016) 98.
[7] X. Zhang, Y. Qu, W. Shen, J. Wang, H. Li, Z. Zhang, S. Li, J. Zho, Physicochem. Eng. Asp. 497 (2016) 280.
[8] A. Merzlyak, S.W. Lee, Curr. Opin. Chem. Biol. 10 (2006) 246.
[9] G. Bagherzade, M. Manzari Tavakoli, M.H. Namaei, Asian Pac. J. Trop. Biomed. 7 (2017) 227.
[10] P. Tippayawat, N. Phromviyo, P. Boueroy, A. Chompoosor, Peer J. 4 (2016) 2589.
[11] C. Pettegrew, Z.D.M. Zubayed Muhi, S. Pease, M. Abdul Mottaleb, M. Rafiq Islam, ISRN Nanotechnology 2014 (2014) 1.
[12] X. Geng T.Z. Grove, RSC Adv. 5 (2015) 2062.
[13] A.G. Kolhatkar, C. Dannongoda, K. Kourentzi , A.C. Jamison, I. Nekrashevich, A. Kar, E. Cacao, U. Strych, I. Rusakova, K.S. Martirosyan, D. Litvinov, T. Randall Lee, R.C. Willson, Int. J. Mol. Sci. 16 (2015) 7535.
[14] M. Vanaja, S. Rajeshkumar, K. Paulkumar, G. Gnanajobitha, C. Malarkodi, G. Annadurai, Int. J. Mater. Biomat. Appl. 3 (2013) 1.
[15] R.R Kannan, R. Arumugam, D. Ramya, K. Manivannan, P. Anantharaman, Appl. Nanosci. 3 (2013) 229.
[16] P. Patil Shriniwas, T. Kumbhar Subhash, Biochem. Biophys. Rep. 10 (2017) 76.
[17] S. Ahmed, B.L. Swami, S. Ikram, J. Adv. Res. 7 (2016) 17.
[18] M. Anbukkarasi, P.A. Thomas, J.R. Sheu, P. Eraldine, Biomed. Pharmacother. 91 (2017) 467.
[19] E.K. Baghkheirati, M.B. Bagherieh-Najjar, Mater. Lett. 171 (2016) 166.
[20] S. Hasani-Ranjbar, B. Larijani, M. Abdollahi, Arch. Med. Sci. 4 (2008) 285.
[21] K. Morteza-Semnani, K. Moshiri, M. Akbarzadeh, J. Essent. Oil Res. 18 (2006) 672.
[22] H. Akhlaghi, A. Motavalizadeh Kakhky, J. Essent. Oil Res. 13 (2010).
[23] M. Deylamsalehi, M. Mahdavi, A. Motavalizadeh Kakhky, M. Akbarzadeh, J. Mahmudi, S.F. Mirahmadi, Z. Ebrahimi, F. Abedi, TEOP J. 16 (2013) 555.
[24] M. Polo, M. Llompart, C. Garcia-Jares, R. Cela, J. Chromatogr. A 1072 (2005) 63.
[25] V. Czitrom, (1999) Am Stat. 53 (1999) 126.

[26] M.A. Bezerra, R.E. Santelli, E.P. Oliveira, L.S. Villar, E.A. Escaleira, L.A. Escaleira, Talanta 76 (2008) 965.
[27] G. Mie, Contributions to the Optics of Turbid Media, Particularly of Colloidal Metal Solutions, Transl. into English from Ann. Phys. (Leipzig) 1976.
[28] D.D. Evanoff, G. Chumanov, Chem. Phys. Chem. 6 (2005) 1221.
[29] J. Rozra, I. Saini, A. Sharma, Mater. Chem. Phys. 134 (2012)1121.
[30] R.R. Banala, V.B. Nagati, P.R. Karnati, Saudi J. Biol. Sci. 22 (2015) 637.
[31] L. Sintubin, W. Verstraete, N. Boon, Biotechnol. Bioeng. 109 (2012) 2422.
[32] M.O. Abdelmageed, M.A. Elsayed, A.M. Elshafei, M.M. Hassan, Genet. Eng. Biotech. 15 (2017) 497.
[33] Montgomery DC. Introduction to Statistical Quality Control: John Wiley & Sons, 2007.